

# Impact of the construction of a filtered tailings stack on top of an existing slurry tailings storage facility at LaRonde gold mine

**E Masengo** *Agnico Eagle Mines, Canada*

**EP Ingabire** *ArcelorMittal, Canada*

**J Huza** *Agnico Eagle Mines, Canada*

**MR Julien** *Agnico Eagle Mines, Canada*

## Abstract

*LaRonde is a gold mine owned and operated by Agnico Eagle Mines since 1988. LaRonde has been depositing slurry tailings in two facilities: the main tailings storage facility (TSF) and Extension A4 TSF. These two facilities reached their full storage capacity at the end of 2022. To accommodate about 12 million tonnes of additional tailings and avoid building a new conventional slurry TSF, LaRonde decided to change their tailings management strategy from slurry tailings to filtered tailings in 2019. The construction of the filtration plant started in April 2020 and was commissioned in October 2022. The selected option for the filtered tailings deposition was to build a filtered tailings stack over the existing Extension A4 TSF. The construction of the filtered tailings stack required the construction of a 1.5 to 2 m-thick waste rock platform (bridgelif) over the slurry tailings within the existing TSF. This paper presents the geotechnical investigation and characterisation of the slurry tailings and the filtered tailings stack, the instrumentation program implemented to monitor the behaviour of the slurry tailings during the construction of the bridgelif and the filtered tailings stack, plus the results of the monitoring program that have been used to verify and update the design assumptions.*

**Keywords:** *filtered tailings, slurry tailings, critical state line, monitoring, inclinometers, porewater pressures*

## 1 Introduction

LaRonde gold mine is owned and operated by Agnico Eagle Mines and is located in the Abitibi region of northwestern Québec, Canada. Since 1988, LaRonde has exploited a polymetallic orebody of gold, silver, zinc, and copper. As of 2023, LaRonde operates LaRonde Zone 5 (LZ5) and LaRonde (LAR) underground mines.

Figure 1 shows a plan view of LaRonde mine waste management infrastructures. Slurry tailings and process water were managed in two tailings storage facilities (TSF) – Main TSF and Extension A4 TSF – and polishing ponds. Main TSF was initially constructed in 1988. It was expanded into the East Extension in 1997. Between 2000 and 2019, Main TSF was incrementally raised to its final elevation of 358 m. Extension A4 TSF was constructed in 2010 to elevation 332 m. Extension A4 TSF is confined by Dike 10, which is a zoned earthfill embankment with a central low permeability till core. Extension A4 TSF covers an area of approximately 68 ha. The maximum height is approximately 22 m at Dike 10 south. Main TSF and Extension A4 TSF reached their full storage capacity with slurry tailings deposition at the end of 2022. LaRonde completed the transition to filtered tailings in October 2022. This paper focuses on the construction of the filtered tailings stack over slurry tailings in Extension A4 TSF.

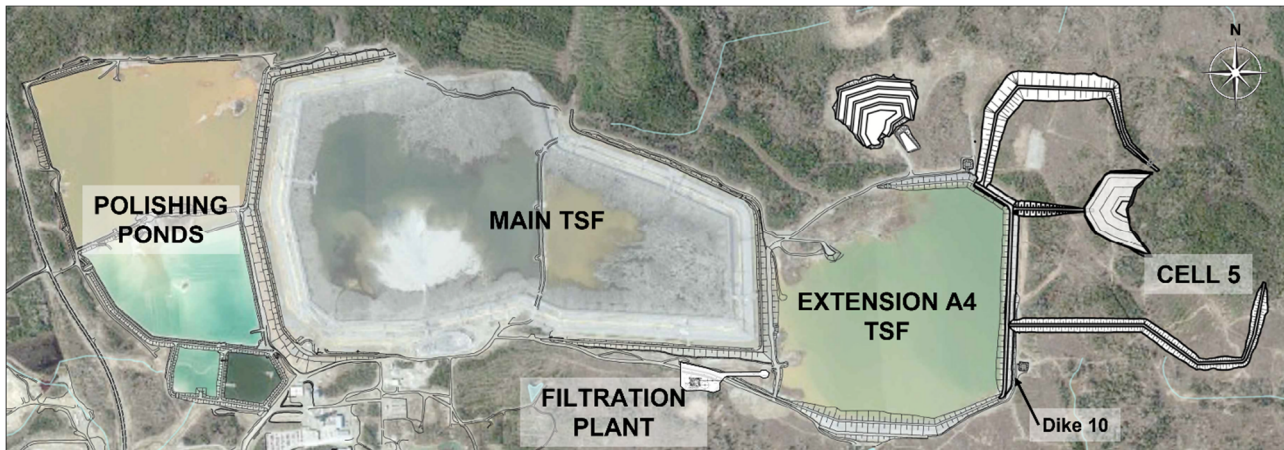


**Figure 1** LaRonde mine waste management infrastructures

## 2 Slurry tailings deposition

Initially, tailings were produced ranging from 25 to 35% solid by mass. Approximately 35 to 40% of the tailings is used for underground cemented paste backfill produced in two paste plants for LZ5 and LAR mines. Therefore, tailings deposition rate can vary daily from about 2,000 t/d, when both paste backfill plants are in operation, to 9,000 t/d when both paste backfill plants are not in operation. On an annual basis, the average tailings deposition rate is approximately 6,000 t/d.

## 3 Transition to filtered tailings

To reduce the risks associated with slurry tailings management, LaRonde transitioned to filtered tailings deposition in October 2022. This change in the tailings management strategy was motivated by:

- The reduction of the environmental footprint by minimising the area impacted by mining activities
- A better management of the physical, environmental, and social risks
- The integration of progressive reclamation during the filtered stack operation.

The transition to filtered tailings required the construction over a three-year period of a filtration plant and a new water management infrastructure, Cell 5, in the vicinity of Extension A4 TSF. Figure 1 shows the location of Extension A4 TSF, the filtration plant, and Cell 5. Details on the construction works completed between April 2020 and October 2022 as part of the transition project are presented in Masengo et al. (2023).

For trafficability purposes, the filtered stack required the construction of a 1.5 to 2.0 m-thick bridgelift composed of waste rock over the slurry tailings. The filtered stack is planned to be constructed to elevation 350 m with 5H:1 V side slopes, in addition to a stability toe berm. The filtered stack will be constructed to its final height sequenced in three different zones – Zone 1 at the south, Zone 2 at the east, and Zone 3 at the northwest – as illustrated in Figure 2. This development strategy allows you to:

- Construct the bridgelift progressively
- Construct the tailings stack at a raising rate which satisfies geochemical and geotechnical stability.
- Limit the tailings exposed area to minimise dust generation
- Start progressive reclamation of the completed zones of the tailings stack
- Update the design and operation of subsequent zones based on the observed previous performance of the filtered stack, slurry tailings, and foundation materials.

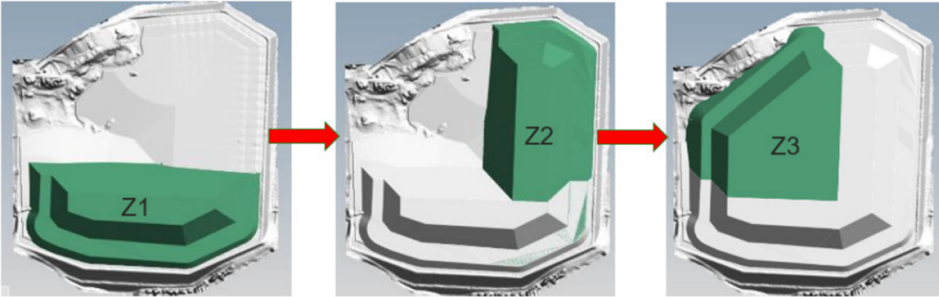


**Figure 2 Development plan of the filtered tailings stack**

Figures 3 and 4 present the construction of the bridgelift and the filtered stack, respectively.



**Figure 3 Bridgelift construction over Extension A4 TSF (September 2023)**



**Figure 4 Filtered tailings stack construction (September 2023)**

## 4 Geotechnical investigations

Between 2019 to 2022, geotechnical investigations were carried out to characterise slurry tailings and cohesive soils in Extension A4 TSF to support the design of the filtered stack. The investigation program included 19 cone penetration tests (CPTs), 17 boreholes, and 12 test pits. At several locations, the CPTs were pushed close to boreholes for calibration purposes. The soundings were advanced to depths between 2.7 and 29.6 m. Shear wave velocity ( $V_s$ ) testing, seismic compression wave velocity ( $V_p$ ) testing, and pore pressure dissipation tests were completed at every CPT location. Field testing also included electronic field vane shear testing (eVST) in the slurry tailings and Nilcon field vane testing (FVST) in the cohesive deposits.

Disturbed tailings samples and high-quality cohesive soil samples were collected for laboratory testing. The laboratory program included index testing for soil identification, and advanced testing to assess consolidation behaviour, hydraulic parameters, critical state parameters, as well as peak and liquefied shear strength parameters.

### 4.1 Subsurface conditions

The general stratigraphy at LaRonde is characterised by glacial till overlying the bedrock. Discontinuous pockets of cohesive soils were identified above the glacial till. Specifically, within the footprint of Extension A4 TSF, subsurface conditions from the surface are as follows:

- An organic layer varying from 0 to 1 m.
- A cohesive soil layer varying from 0 to 11 m.
- A till layer varying from 0 to 14 m.
- Bedrock.

The thickest clayey layer is located in the northern section of Dike 10 East. The cohesive soil thickness varies between 5 to 6 m below the footprint of the northern section of Dike 10 East and between 1 to 3 m below the footprint of Dike 10 south. The varved cohesive deposit varies from a low-plasticity silt (ML) to clay (CH). In the upper 2 to 3 m, an over-consolidated crust is noted, below which the clays are generally normally consolidated with a water content higher than the liquid limit and a liquidity index higher than 1.0. Results from FVSTs indicate a soft to firm consistency in the normally consolidated clays.

The thickest till layer is located in the northern section of Dike 10 East. The till varies from a sandy silt to silty sand to sand and gravel. The till layer is compact to very dense from results of standard penetration tests. Dike 10 rests locally on bedrock, at the east and west corners of Dike 10 south, and at Dike 10 north.

### 4.2 Slurry tailings characterisation

#### 4.2.1 Materials tested

The various mining zones exploited during the history of LaRonde result in heterogeneity of the slurry tailings. Moreover, tailings segregate with depth and with distance from Dike 10 due to the temporal variations in the deposition. Slurry tailings within Extension A4 TSF can be described as a non-plastic silty sand (SM) to ML. Fines content ( $FC$ ) varies between 35 to 100% for LAR tailings. LZ5 are generally finer, with  $FC \geq 95\%$ .

#### 4.2.2 Cone penetration test signature

Figure 5 shows the normalised cone resistance ( $Q$ ) and pore pressure ratio ( $B_q$ ) profiles obtained from CPTs along a cross-section of Dike 10 south. Tailings segregation is apparent by analysing the CPT signatures. Fine-grained tailings show a lower tip resistance and exhibit excess porewater pressure during cone penetration ( $B_q > 0.1$ ). From analysis of the particle size distribution and CPT signatures, slurry tailings were separated in four representative materials: LZ5 tailings, LAR-fine tailings, LAR-medium tailings, and



LAR-coarse tailings. Table 1 provides a summary of the index properties of LAR and LZ5 tailings within Extension A4 TSF.

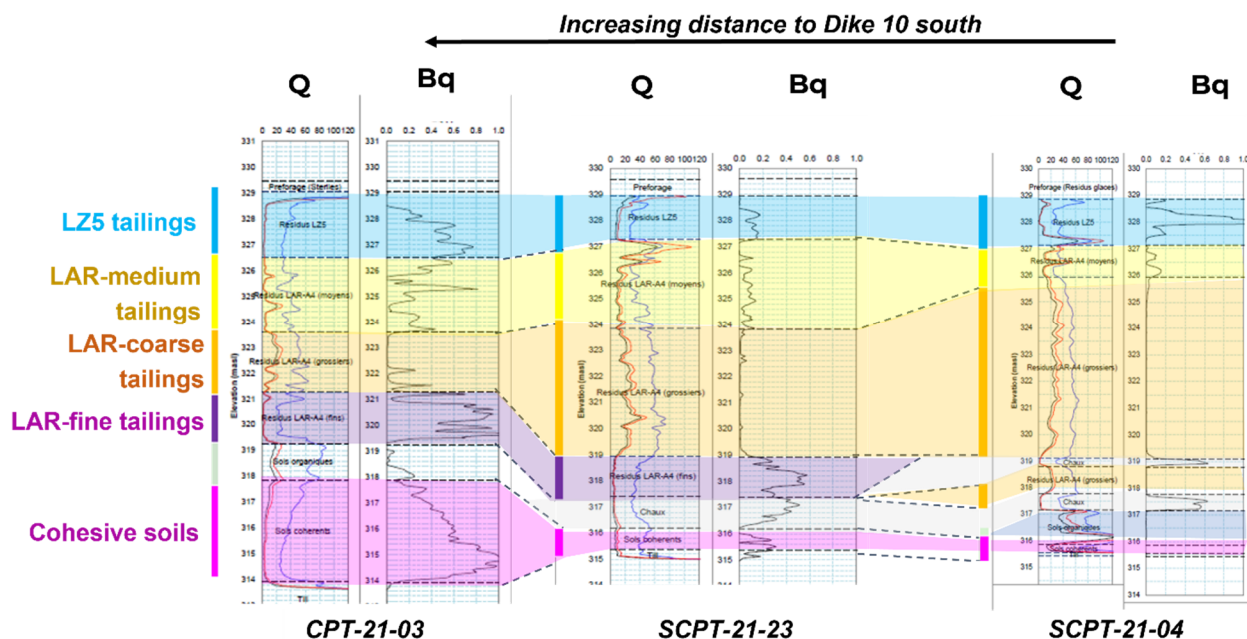


Figure 5 Cone penetration tests along one cross-section of Dike 10 south

Table 1 Index properties of LZ5 and LAR tailings

Material	Fines content, $FC$ (%)	$D_{10}$ (mm)	$D_{50}$ (mm)	$D_{90}$ (mm)	$G_s$
LZ5	98	0.002	0.015	0.055	3.00
LAR-fine	95	0.006	0.03	0.07	3.35
LAR-medium	70	0.01	0.05	0.12	3.31
LAR-coarse	50	0.03	0.07	0.17	3.20

### 4.2.3 Critical state parameters

Further advanced laboratory testing was completed on the representative materials which had the most influence on the stability assessment of the filtered stack: LZ5, LAR-fine, and LAR-medium. For each of these materials, six to nine triaxial tests were conducted to determine their critical state lines (CSL). Triaxial specimens were reconstituted by moist tamping to achieve a wide range of initial void ratios. Specimens were isotropically or anisotropically consolidated to a range of confining stresses varying from 50 to 500 kPa. Once consolidated, the specimens were sheared under both drained and undrained conditions. To accurately measure the void ratio, the specimens were frozen at the end of the test.

The CSL is often represented in a semi-logarithmic space. The parameters that define the CSL are its intercept at a mean effective stress ( $p'_{cs}$ ) of 1 kPa ( $\Gamma$ ) and slope ( $\lambda_{10}$ ).  $M_{tc}$  is the critical shear stress ratio and is analogous to the critical state friction angle ( $\phi_{cs}$ ).

$$e_{cs} = \Gamma - \lambda_{10} \log(p'_{cs}) \tag{1}$$

$$M_{tc} = \frac{q_{cs}}{p_{cs}} \tag{2}$$

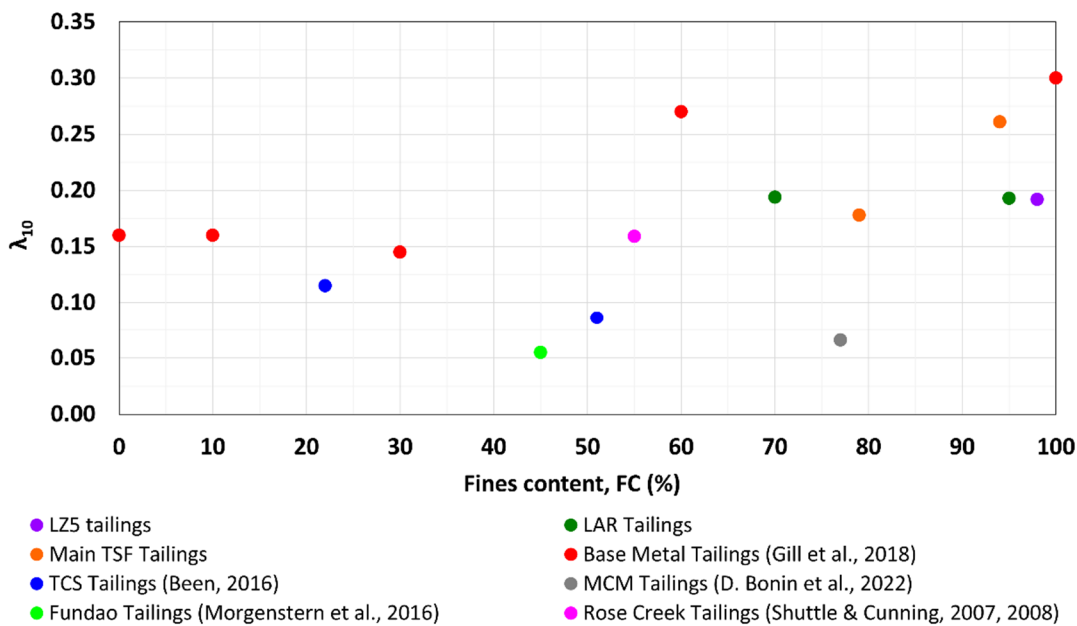
$$\sin \phi_{cs} = \frac{3M_{tc}}{6 + M_{tc}} \tag{3}$$

Table 2 presents the critical state parameters determined for LZ5, LAR-fine, and LAR-medium tailings. In Table 2, the value of  $\lambda_{10}$  is similar for all tailings, regardless of their origin or  $FC$ . In Figure 6, values of  $\lambda_{10}$

and  $FC$  are plotted for LZ5 and LAR tailings, as well as Main TSF tailings and other tailings available in the literature (Been 2016; Bonin et al. 2022; Gill et al. 2018; Morgenstern et al. 2016; Shuttle & Cuning 2007, 2008). There is no direct trend between increasing  $FC$  and increasing  $\lambda_{10}$ , which suggests that  $FC$  may not be a direct proxy for compressibility similarly to the observations of Ingabire et al. (2019).

**Table 2 Critical state parameters**

Material	Fines content, $FC$ (%)	$\Gamma$	$\lambda_{10}$	$M_{tc}$	$\phi_{cs}$ (°)
LZ5	98	1.29	0.192	1.43	35
LAR-fine	95	1.31	0.193	1.36	34
LAR-medium	70	1.15	0.194	1.36	34



**Figure 6 Influence of fines content,  $FC$ , on  $\lambda_{10}$**

#### 4.2.4 *In situ state*

The in situ state parameter ( $\psi$ ) was calculated using screening methods (e.g. Plewes et al. 1992) and NorSand calibration and the cavity expansion analysis (Jefferies & Been 2015; Shuttle & Jefferies 2016). Table 3 presents the variation in the calculated  $\psi$  depending on the method chosen. Results indicate a contractive state ( $\psi_k > -0.05$ ) for all the tailings within Extension A4 TSF. Comparison shows that the screening method gives a more conservative estimate of  $\psi_k$  (e.g. looser state). LAR-coarse tailings show a denser state than LAR-medium and LAR-fine tailings.

**Table 3 Characteristic state parameter of tailings**

Method	LZ5	LAR-fine	LAR-medium	LAR-coarse
Plewes et al. (1992)	0.14	0.16	0.09	-0.01
Shuttle & Jefferies (2016)	–	0.12	0.04	–

#### 4.2.5 *Undrained strength parameters*

As the in situ state of slurry tailings within Extension A4 TSF was found contractive, particular attention was given to the assessment of the peak and liquefied undrained shear strength ( $s_u$ ). Given the complexity in

assessing  $s_u$  for sand-like transitional materials, the methodology adopted relied on both in situ and laboratory data.

Undrained shear strengths were evaluated from calibration of the CPT with eVST results and screening methods (e.g. Robertson 2010). Laboratory-based  $s_u - \psi$  correlations were developed by testing samples in the triaxial and direct simple shear apparatuses and from numerical simulation (Jefferies & Been 2015). CPT is then used to estimate the in situ state and indirectly estimate shear strength.

Applicability of vane testing and empirical screening methods on sandy/silty tailings could be questioned because of discussions around partial drainage during the vane rotation or the limited dataset of back-calculated strengths. The laboratory-based framework poses the challenge of not being able to test samples representative of field conditions as it is not practical to retrieve undisturbed tailings samples in practice. The authors believe that each method has its merits and that the results of each method should be compared whenever practical to do so.

## 5 Stability assessment

Stability of the filtered tailings stack and Dike 10 was evaluated at each stage of filtered tailings deposition. The limit-equilibrium and load-deformation models were used to refine the rate of deposition and the geometry of the filtered tailings stack and buttressing toe berms to achieve the desired Factors of Safety (FoS). The potential failure surfaces considered for the stability assessment – Surface 1 passing in the foundation beneath the starter dike and Surface 2 through the crest of the filtered stack, daylighting upstream of the starter dike – are shown in Figure 7.

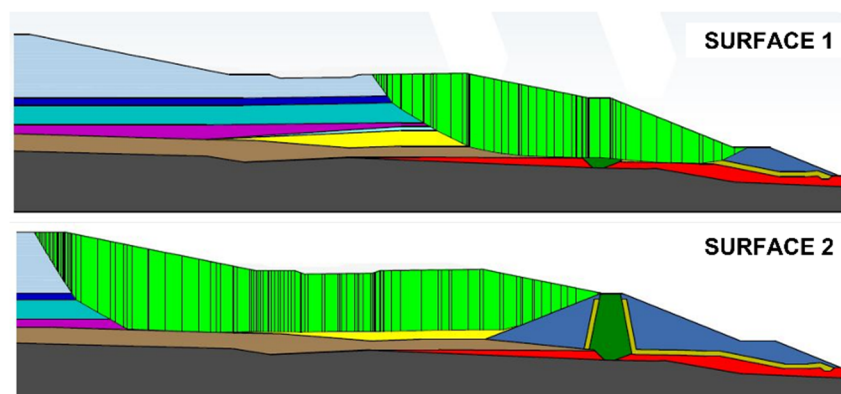


**Figure 7** Potential failure surfaces considered in the stability assessment

Slope stability analyses were completed to assess post-construction ‘steady-state’ FoS at critical cross-sections. At the final stage of deposition, the model includes the bridgelift, the filtered tailings stack at an elevation of 350 m, and buttressing toe berms for the filtered stack and the starter dike. Results of stability assessment for different cross-sections considered are presented in Table 4.

**Table 4** Results of stability assessment for the final configuration of the tailings stack at an elevation of 350 m

	CS2	CS3	CS4
Static condition (target Factor of Safety > 1.5)			
Surface 1	1.5	1.8	1.9
Surface 2	1.7	1.7	1.7
Post-liquefaction condition (target Factor of Safety > 1.3)			
Surface 1	1.4	1.7	1.4
Surface 2	1.3	1.3	1.4

Short-term conditions considering load-induced porewater pressures from placement of filtered tailings and temporary elevated groundwater table were considered as part of the load-deformation analyses. The analyses simulate excess porewater pressure development (and temporary reduction of FoS) and subsequent porewater pressure dissipation (and increase of FoS) in the stack, slurry tailings, and cohesive soils during each stage of filtered tailings deposition. The construction of the tailings stack must allow pressures to dissipate such that the targeted 'steady-state' FoS is achieved prior to placement of a subsequent lift.

Considering the development sequence illustrated in Figure 2 and the required storage capacity, it is evaluated that the stack will be raised at an average rate of about 0.7 m/month. It is planned that the filtered tailings will be placed in lifts of a maximum thickness of 0.5 m to achieve a minimum of 95% standard maximum dry density.

Figure 8 illustrates the response predicted by the load-deformation model in the filtered and slurry tailings and cohesive soils during construction in Zone 2. An overall increase in excess porewater pressure during the 29 months of deposition is noted, with small decreases during each of the rest periods. Following the 29 months of deposition, excess porewater pressures gradually decrease. Engineering of the filtered stack includes the development of contingency deposition plans which could be implemented if porewater pressure generation is higher than anticipated.

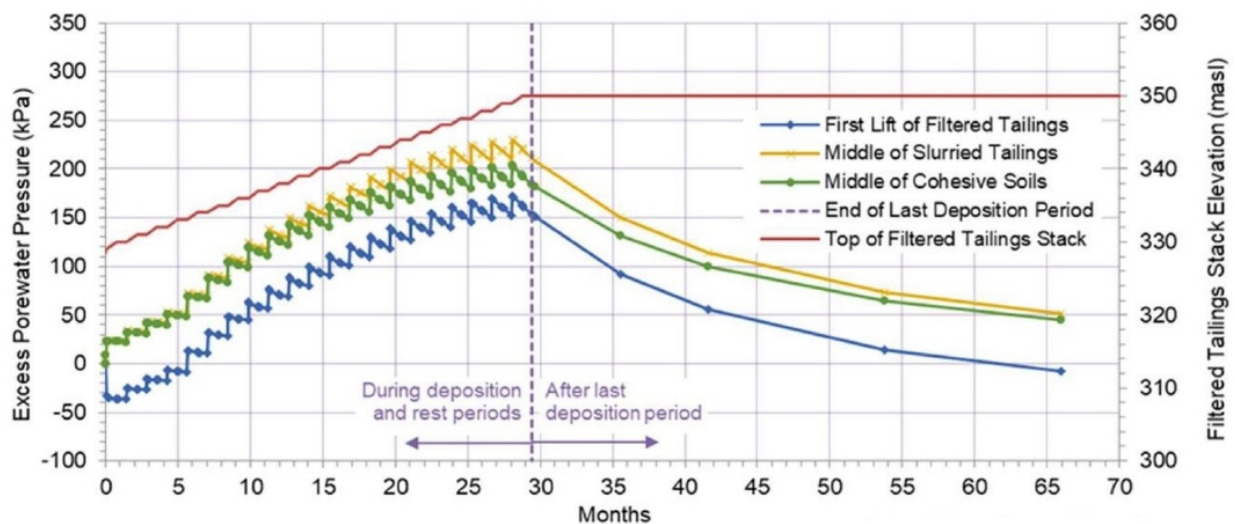


**Figure 8** Response in the filtered and slurry tailings and cohesive soils during construction in Zone 2

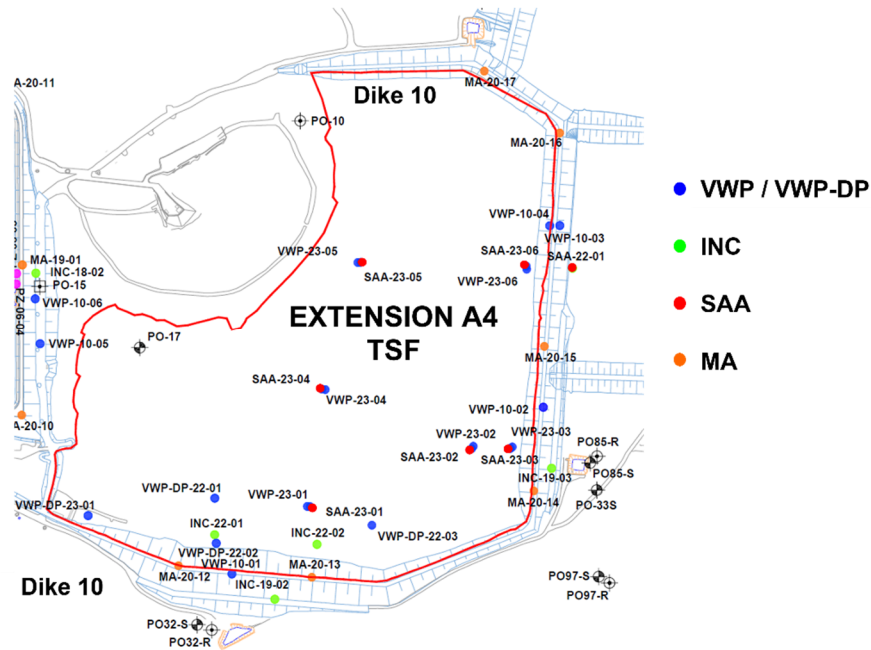
## 6 Instrumentation and monitoring

LaRonde site personnel was responsible for the monitoring and the surveillance activities. The management and the governance applied at the site allows the development of in-house capabilities and favours the ownership of the team while reducing the risks related to the construction of the filtered tailings stack.

Figure 9 provides the location of the instruments installed to monitor the construction of the bridgelifft and the filtered tailings stack. The instruments include:

- Vibrating wire piezometers (VWPs) and drive-point VWPs (VWP-DP) at different depth in the slurry tailings and in the foundation
- Inclometers (INCs) located upstream of Dike 10 to monitor the deformations in the slurry tailings underneath the bridgelifft and the filtered tailings stack
- INCs located downstream of Dike 10 to monitor the deformation at the toe
- Shape array accelerometers (SAAs) located upstream and downstream of Dike 10, similarly to INCs
- Settlement plates (MA) to monitor consolidation of the slurry tailings and settlement of the crest of the stater dam.

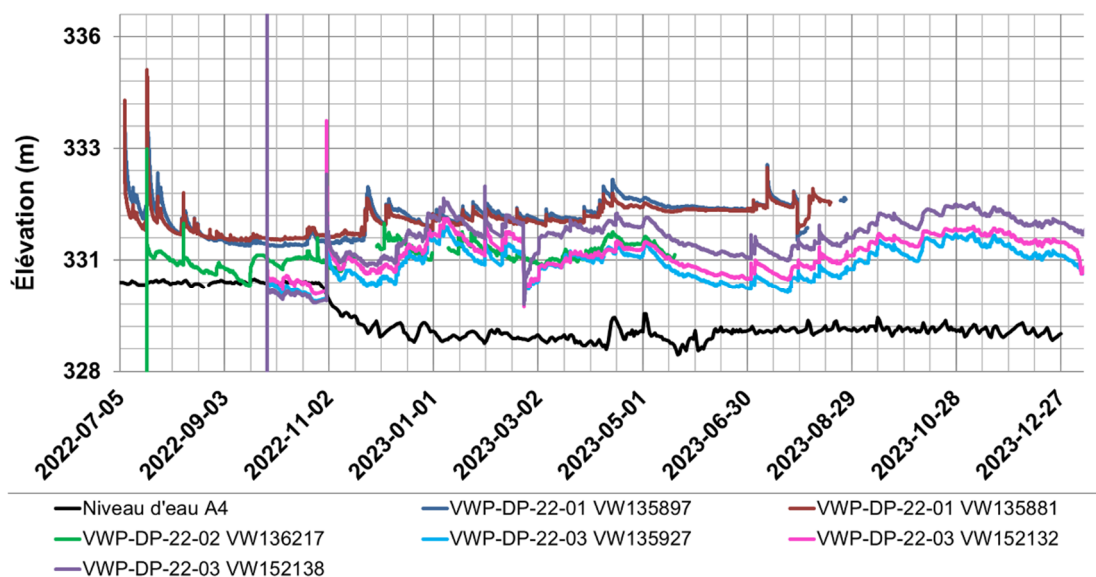




**Figure 9** Location of the instruments within Extension A4

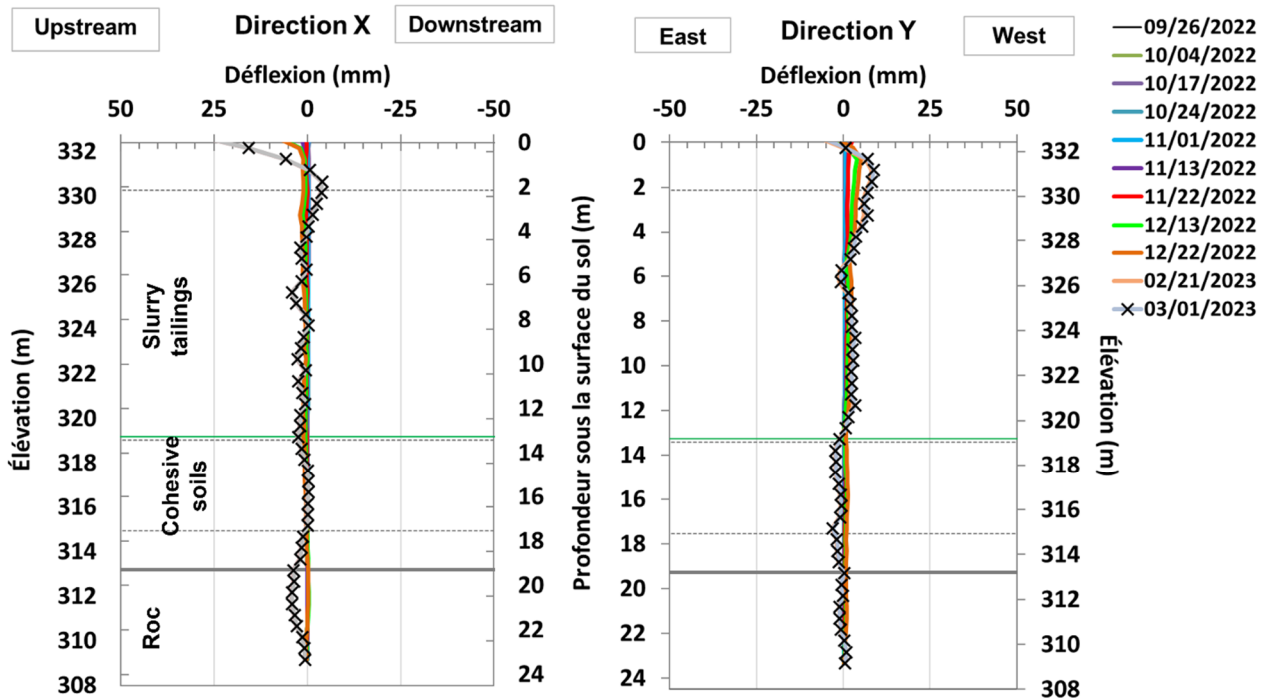
The VWPs and VWP-DPs are connected to data loggers or other automated systems to allow for frequent readings and remote data collection. Data from INCs are collected manually on a regular basis but SAAs are automated instruments which can be read frequently and allow remote data collection.

Figure 10 shows typical data collected from the VWP-DPs between July 2022 and December 2023. The readings in the slurry tailings indicate that excess porewater pressures are increasing during the placement of the bridgelift and/or a layer of filtered tailings but dissipate relatively fast during the resting period when the zone of construction activities changes. The occasional high spikes indicate the excess porewater pressures induced by the loading tests followed by relatively fast dissipation. The frequent lower spikes correspond to the placement of a filtered tailings layer followed by a dissipation during the resting period that could vary up to more than two weeks. Therefore, it could be considered that the construction rate is slow enough to allow relatively fast dissipation of excess porewater pressures after each lift followed by a rest period of about two weeks.



**Figure 10** Porewater pressure monitoring during construction in Zone 1

Figure 11 provides typical data collected from the inclinometers between September 2022 and March 2023. No data has been collected from the SAA yet because they have been installed recently. No significant lateral bulging was observed in the slurry tailings during the construction of the bridgelift; however, it is expected to occur as the construction of the filtered tailings stack progresses and its height/weight increases inducing more consolidation and deformations in the slurry tailings.



**Figure 11 Inclinometers monitoring during construction in Zone 1**

Instrumentation and monitoring will be updated periodically, and new instruments will be installed as the construction of the filtered tailings stack continues and its height increases.

## 7 Large-scale loading tests

To verify and inform design parameter selection, three large-scale loading tests were completed in Zone 1. Two tests were completed on 31 October 2022 and 30 January 2023 at the location of VWP-DP-22-03. An additional test was also completed on 1 March 2023 at the location of INC-22-02. Note that the first test at VWP-DP-22-02 location was carried out directly on the bridgelift before the placement of the filtered tailings while the second test was carried out after the placement of 3 m of filtered tailings.

At the location of VWP-DP-22-03, three VWPs were installed in the slurry tailings: 1 VWP in LZ5 tailings (at 3.2 m depth), 1 VWP in LAR-coarse tailings (at 6.0 m depth), and 1 VWP in LAR-fine tailings (at 8.4 m depth). A 2.8 m-high waste rock load was placed in a relatively short time (instantaneous load) to attempt to simulate undrained conditions and to monitor the generation and dissipation of the excess porewater pressures (PWP) in the slurry tailings. Readings were recorded every minute during the test.

Figure 12 illustrates a schematic of the loading test at the location of VWP-DP-22-03 with the VWP depths measured from the bottom of the bridgelift.

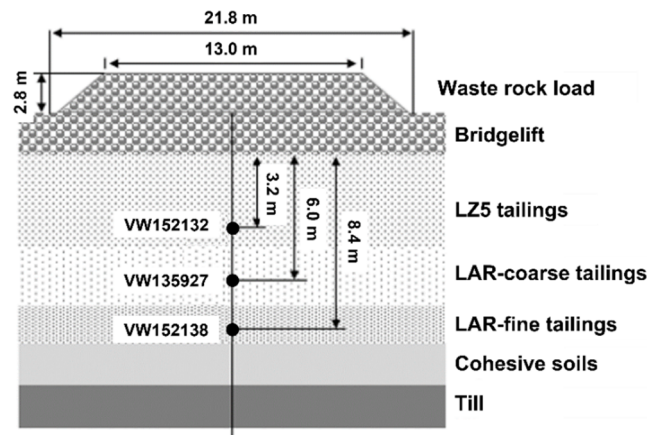


**Figure 12 Schematic of the large-scale field loading test at the location of VWP-DP-22-03**

Table 5 shows the PWP coefficient ( $\bar{B}$ ) and PWP ratio ( $R_u$ ) calculated during the three loading tests.  $\bar{B}$  is defined as

$$\bar{B} = \frac{\Delta u}{\Delta \sigma} \quad (4)$$

where:

$\Delta u$  = PWP increase due to the applied load

$\Delta \sigma$  = stress increase at each VWP depth.

$\Delta \sigma$  was estimated using Boussinesq equation.  $R_u$  is defined as

$$R_u = \frac{u}{\sigma_v} \quad (5)$$

where:

$u$  = PWP reading following the loading test

$\sigma_v$  = total vertical stress at each VWP depth.

**Table 5 Porewater pressure coefficient ( $\bar{B}$ ) and porewater pressure ratio ( $R_u$ ) during the large-scale loading tests at the location of VWP-DP-22-03 and INC-22-02**

Vibrating wire piezometer (VWP) ID	VWP depth (m)	Material	$\bar{B}$ (-)	$R_u$ (-)
VWP-DP-22-03, on 31 October 2022				
VW152132	3.2	LZ5 tailings	0.65	0.40
VW135927	6.0	LAR-coarse tailings	0.55	0.35
VW152138	8.4	LAR-fine tailings	0.70	0.40
VWP-DP-22-03, on 30 January 2023				
VW152132	3.2	LZ5 tailings	0.38	0.22
VW135927	6.0	LAR-coarse tailings	0.34	0.27
VW152138	8.4	LAR-fine tailings	0.51	0.34
INC-22-02 on 1 March 2023				
VW149665	7.0	Slurry tailings	0.45	0.24
VW149699	12.0	Slurry tailings	0.58	0.31
VW149920	15.5	Cohesive soils	0.66	0.31
VW149687	18.5	Till	N/A	N/A

In Table 5,  $\bar{B}$  in the cohesive soils is higher than in the slurry tailings.  $\bar{B}$  values are between 0.5 and 0.7 which was found to be encouraging as these values suggest partially drained conditions.  $\bar{B}$  values are higher in LAR-fine tailings compared to LAR-coarse and LZ5 tailings, which fits well with the interpretation of the CPT signatures shown in Figure 5.  $R_u$  values in the slurry tailings and the cohesive soils vary between 0.2 and 0.4. An  $R_u$  threshold value of 0.7 is generally considered as an onset value for liquefaction (Sadrekarimi 2014) in the tailings and the results are well below this value.

Figure 13 illustrates the PWP variation caused by the loading test at the location of VWP-DP-22-03 on 31 October 2022. The data show a sudden increase followed by PWP dissipation. Detailed results on the loading test at the location of INC-22-02 on 1 March 2023 are presented in Masengo et al. (2023).

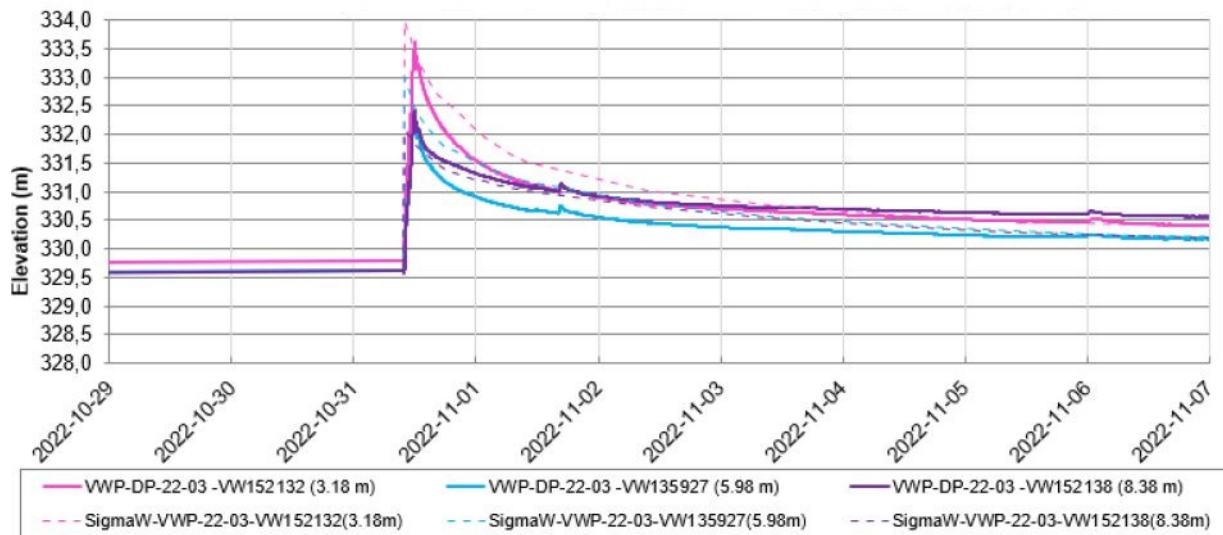


**Figure 13 Porewater pressure variation caused by the large-scale loading tests at the location of VWP-DP-22-03 on 31 October 2022**

In Figure 13, a positive agreement is obtained between the measured porewater pressures (shown by the solid lines) and the prediction of the load-deformation model (shown by the dotted lines). The model generally overestimates the sudden increase in PWP. In the short-term (24 hours), the rate of PWP dissipation is slightly lower in the model than in the field. In the long-term (after 7 days), the rate of dissipation is equal or slightly greater in the model than in the field. Overall, results from the load tests confirm the value of hydraulic conductivity determined by interpretation of the pore pressure dissipation tests during CPT. The large-scale loading tests have indicated that the excess porewater pressures dissipate relatively fast; this type of tests will continue to be carried out throughout the construction period to appraise future behaviour.

## 8 Conclusion

LaRonde gold mine transitioned to filtered tailings deposition in October 2022 with a filtered tailings stack to be constructed over Extension A4 TSF, an existing slurry tailings TSF. This change in the tailings management strategy was mainly motivated by the reduction of the environmental footprint and the societal risks, and by the possibility to integrate progressive rehabilitation during the construction of the filtered stack.

An exhaustive investigation program was completed between 2019 to 2022. The program included in situ testing and advanced laboratory testing to characterise the slurry tailings and cohesive soils within the footprint of Extension A4 TSF. The results of the investigation were used to inform the design of the filtered stack.

Given that the slurry tailings are contractive, it was assumed that they will liquefy. Therefore, stability analyses were carried out on the filtered tailings stack using liquefied shear strength parameters. The results



indicate that the minimum required Factor of Safety would be satisfied if liquefaction occurred in the slurry tailings.

Supported by the designer and the engineer of record, LaRonde developed a monitoring and surveillance program for the construction of the bridgelifit and the filtered tailings stack. Readings from geotechnical instruments are used to update the operations and the design. The performance of the instrumentation is very good which has allowed to collect a significant amount of reliable data that will be used to calibrate the load-deformation model.

Instrumentation and monitoring will be updated periodically and new instruments will be installed as the construction of the filtered tailings stack continues and its height increases. So far, the vibrating wire piezometer readings suggest that the construction rate is slow enough to allow relatively fast dissipation of excess porewater pressures after each lift. Inclinator readings do not show significant lateral bulging, although it is expected to occur as the construction of the filtered tailings stack progresses. Based on instrument readings and visual observations during construction, it can be considered that the slurry tailings underneath the bridgelifit and the filtered tailings stack behaved as expected during this first year of filtered tailings deposition.

The large-scale loading tests have indicated that the excess porewater pressures dissipate relatively fast. Results from the large-scale loading tests agree quite well with the load-deformation model. Large-scale loading tests will continue to be carried out to appraise future behaviour.

## Acknowledgement

The authors acknowledge the contribution of LaRonde tailings management team in the success of the filtered tailings stack construction: Yanick Létourneau, Patrick Laporte, Francis Guay, and René Lavallière.

## References

- Been, K 2016, 'Characterizing mine tailings for geotechnical design', in BM Lehane, HE Acosta-Martinez & R Kelly (eds), *Proceedings of the Geotechnical and Geophysical Site Characterisation 5*, Australian Geomechanics Society, Sydney, pp. 59–78.
- Bonin, MD, Limoges Shaiget, M, El Takch, A, Becker, DE & Masengo, E 2022, 'In-situ and laboratory site specific geotechnical characterization of hard rock gold mine tailings', *Tailings and Mine Waste 2022*, Colorado State University, Denver.
- Gill, S, Ingabire, EP, Vipulanathan, M, Siu, M, Clelland, L, Sy, A & Ghafghazi, M 2018, 'Influence of fines content on interpretation of CPT tip resistance for liquefaction assessment in mine tailings', *GeoEdmonton 2018: 72nd Canadian Geotechnical Conference*, Edmonton.
- Ingabire, EP, Clelland, L, Sy, A & Ghafghazi, M 2019, 'Influence of fines content on cyclic resistance through the critical state framework', *GeoStJohns 2019: 73rd Canadian Geotechnical Conference*, St-Johns.
- Jefferies, M & Been, K 2015, *Soil Liquefaction: A Critical State Approach*, 2nd edn, CRC Press, Abingdon.
- Masengo, E, Ingabire, EP, Boily, S, Létourneau, Y, Laporte, P, Guay, F, ... Julien, MR 2023, 'Transition to filtered tailings at LaRonde Gold Mine', *Tailings and Mine Waste 2023*, Colorado State University, Denver.
- Morgenstern, NR, Vick, SG, Viotti, CB & Watts, BD 2016, *Fundão Tailings Dam Review Panel: Report In The Immediate Causes Of The Failure of the Fundão Dam*, Cleary Gottlieb Steen & Hamilton LLP.
- Plewes, HD, Davies, MP & Jefferies, MG 1992, 'CPT based screening procedure for evaluating liquefaction susceptibility', *45th Canadian Geotechnical Conference*, Canadian Geotechnical Society, Toronto.
- Robertson, PK 2010, 'Evaluation of flow liquefaction and liquefied shear strength using the cone penetration test', *Journal of Geotechnical and Geoenvironmental Engineering*, vol. 136, no. 6, pp. 842–853, [https://doi.org/10.1061/\(ASCE\)GT.1943-5606.0000286](https://doi.org/10.1061/(ASCE)GT.1943-5606.0000286)
- Sadrekarimi, K 2014, 'Effect of the mode of shear on static liquefaction analysis', *Journal of Geotechnical and Geoenvironmental Engineering*, vol. 140, no. 2, [https://doi.org/10.1061/\(ASCE\)GT.1943-5606.0001182](https://doi.org/10.1061/(ASCE)GT.1943-5606.0001182)
- Shuttle, DA & Cunning, J 2007, 'Liquefaction potential of silts from CPTu', *Canadian Geotechnical Journal*, vol. 44, no. 1, pp. 1–19, <https://doi.org/10.1139/t06-086>
- Shuttle, DA & Cunning, J 2008, 'Reply to the discussion by Robertson on 'Liquefaction potential of silts from CPTu'', *Canadian Geotechnical Journal*, vol. 45, no. 1, pp. 142–145, <https://doi.org/10.1139/T07-119>
- Shuttle, DA & Jefferies, M 2016, 'Determining silt state from CPTu', *Geotechnical Research*, vol. 3, no. 3, pp. 90–118, <https://doi.org/10.1680/jgere.16.00008>

